CORE
Metadata, citation and similar papers at core.ac.uk
Provided by University of Queensland eSpace

Biodegradable Core Crosslinked Star Polymer Nanoparticles as ^{19}F MRI Contrast Agents for Selective Imaging

Kewei Wang, , Hui Peng, Kristofer J. Thurecht, Simon Puttick and Andrew K. Whittaker*

Received (in XXX, XXX) Xth XXXXXXXXX 20XX, Accepted Xth XXXXXXXXX 20XX
DOI: 10.1039/b000000x

With the aim of developing stimuli-responsive imaging agents, we report here the synthesis of core crosslinked star (CCS) polymers and their evaluation as pH-sensitive ^{19}F magnetic resonance imaging (^{19}F MRI) contrast agents. Block copolymers consisting of poly(ethylene glycol) methyl ether methacrylate (PPEGMA) as the first block and a copolymer of 2-(dimethylamino)ethyl methacrylate (DMAEMA) and 2,2,2-trifluoroethyl methacrylate (TFEMA) as the second block were synthesised using RAFT polymerisation. The polymerisation kinetics were studied in detail. The block copolymers were then used as arm precursors for the arm-first synthesis of CCS polymers through RAFT dispersion polymerisation. The synthetic conditions were investigated and optimised. CCS polymers with a degradable core were also synthesised and evaluated as ^{19}F MRI contrast agents. The degradation of the core was confirmed by treatment with various reducing agents. The particle size, ^{19}F NMR signal and relaxation times as well as ^{19}F MRI imaging performance of the CCS polymers were studied at a range of value of solution pH. Significant enhancement of the image intensity was observed when the pH was decreased from 8 to 5, indicating that the CCS nanoparticles could be used as ^{19}F MRI contrast agents for the detection of the acidic environment within tumour tissue.

Introduction

Magnetic resonance imaging (MRI), a commonly-used diagnostic modality, has proven to be an indispensable imaging technique since its first appearance in the early 1970s. Unlike other imaging procedures, in particular X-ray computed tomography (CT), MRI does not utilise ionizing radiation during image acquisition, and is therefore non-harmful to humans. ^{1}H MRI in particular can provide spatial anatomical images with high quality and resolution, with contrast arising from differences in proton density and relaxation parameters. However, ^{1}H MRI is intrinsically restricted by two factors. First, the abundant water molecules in the body generate strong background signals that make detection of small concentrations of particular tissue types or metabolites difficult. Secondly, the proton relaxation times in different tissues are often similar, resulting in poor image contrast.[1] To address these issues, tremendous efforts have been devoted to the development of ^{1}H MRI contrast agents. The principle classes of ^{1}H MRI contrast agents include gadolinium-based chelates,[2-4] superparamagnetic iron oxide nanoparticles,[5, 6] manganese-based contrast agents,[7-11] and other lanthanide-based contrast agents.[12, 13] An alternative approach to improving image contrast is to consider other NMR-active nuclei, and ^{19}F MRI has been considered to be an excellent option.

Australian Institute for Bioengineering and Nanotechnology and Centre for Advanced Imaging, The University of Queensland, St Lucia, 4072, Australia. E-mail: a.whittaker@uq.edu.au; Fax: +61-7-33463973; Tel: +61-7-33463885

† Electronic Supplementary Information (ESI) available: [GPC, DLS and NMR results]. See DOI: 10.1039/b000000x/

Shortly after the appearance of ^{1}H MRI, the first example of ^{19}F MRI was reported in 1977.[14] Compared to other candidates, such as ^{13}C, ^{15}N and ^{31}P, the ^{19}F nucleus exhibits a number of attractive properties, e.g. 100% natural abundance, high sensitivity (83% relative to ^{1}H), large gyromagnetic ratio (40.03 MHz/T, 94% relative to ^{1}H), and absence in the human body.[15-17] The physiological rarity of mobile fluorine nuclei in the body guarantees essentially no background signal during imaging and highlights the distinctive advantage of ^{19}F MRI. ^{19}F MRI naturally relies on the use of ^{19}F-containing contrast agents, and a high concentration of ^{19}F nuclei is preferred in the target voxel to provide adequate signal for the acquisition of good quality images. During the past few decades, perfluorocarbons (PFCs) have been extensively exploited as ^{19}F MRI contrast agents because of their high fluorine content as well as chemical and biological inertness.[17-19] Due to their hydrophobicity, PFCs are normally formulated as emulsions for biological applications. Although a few PFCs emulsion are commercially available for clinical use, this category of contrast agents has several drawbacks, such as emulsion stability, limited methods of functionalization and long reticuloendothelial system clearance times.[20-22]

Recently, ^{19}F MRI contrast agents based on polymers have been introduced by a number of groups. Several classes of polymeric agents have been developed and evaluated, including linear polymers,[23-28] hyperbranched polymers,[29, 30] dendrimers[31-34] and

This is a post-print version of the following article: Wang, Kewei, Peng, Hui, Thurecht, Kristofer J., Puttick, Simon and Whittaker, Andrew K. (2014) Biodegradable core crosslinked star polymer nanoparticles as 19F MRI contrast agents for selective imaging. *Polymer Chemistry*, *5* 5: 1760-1771.

nanogels.[35] In our previous studies, we suggested that polymeric ^{19}F MRI agents should fulfil a list of criteria, i.e. high fluorine content, separation of fluorine segments, small particle size, low cytotoxicity and possibility for chemical modification of conjugation.[24, 25, 30] We are particularly interested in polymeric contrast agents that have highly-branched structures because these polymers have the potential to fulfil the aforementioned requirements. In these molecules, a high concentration of highly separated fluorine segments retains high flexibility, resulting in efficient averaging of the dipolar coupling and therefore ensures strong signal intensity in ^{19}F MRI. On the other hand, the abundant functional groups in the polymers are especially favourable for

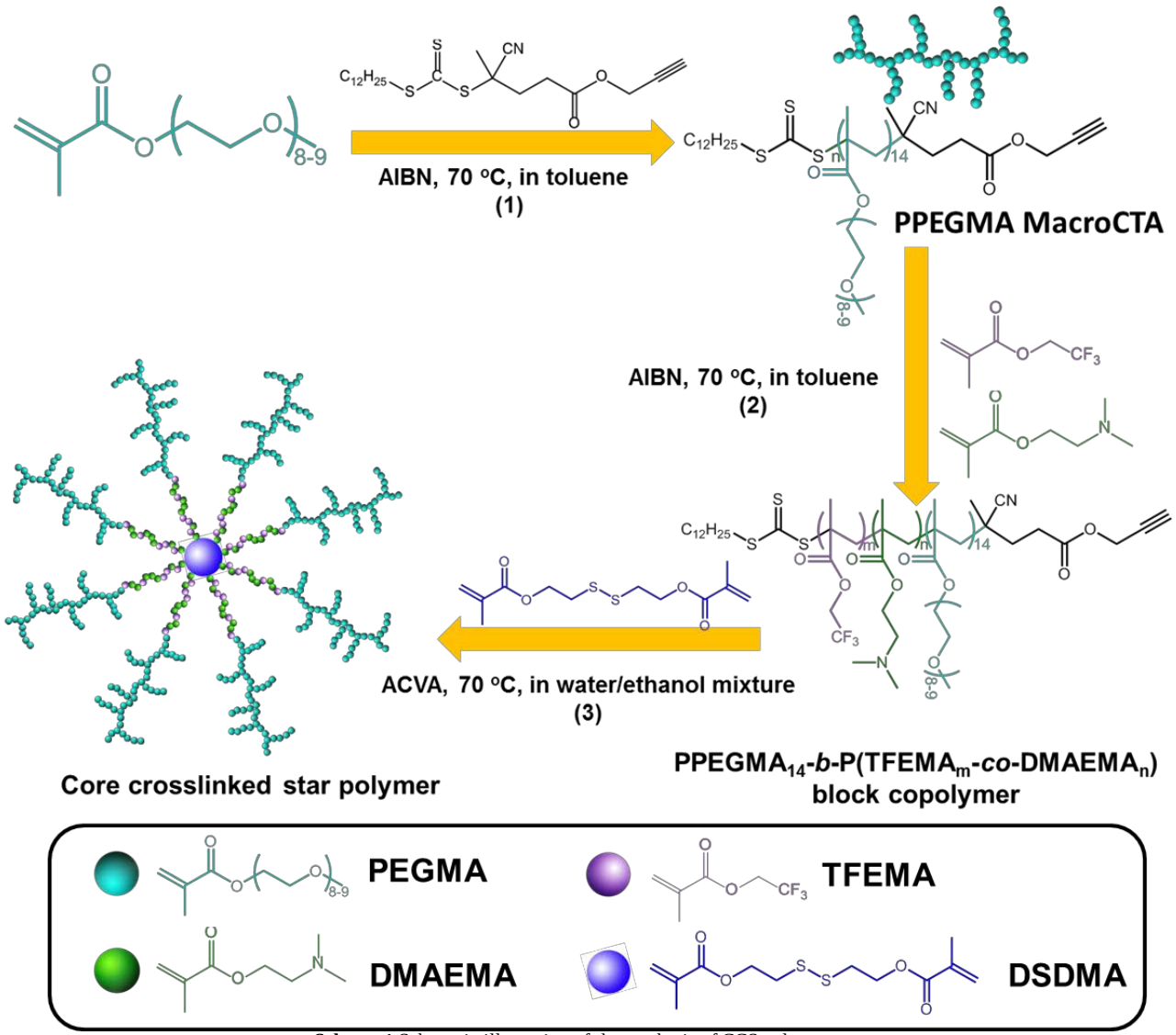

Scheme 1 Schematic illustration of the synthesis of CCS polymers

subsequent functionalization for specific applications.

In recent years 'smart' imaging agents, which are responsive to certain environmental conditions (pH, temperature, light, ionic strength, the presence of enzymes, redox potential, etc.), have elicited great scientific interest.[36-42] In particular it is well known that compared to normal tissues, cancerous tissues have a slightly acidic extracellular pH (6.7-7.1),[43] hence it has been suggested that they may be detected through selective imaging using contrast agents that can be triggered by a change in pH. The development of pH-responsive imaging agents has become an intensive research field, and a variety of such imaging agents have been fabricated and show great potential for the early diagnosis of cancer diseases.[34, 44-50].

Core crosslinked (CCS) star polymers, which are composed of a number of arms and a crosslinker core, have a spherical 3D structure and possess unique properties. In the past several years, CCS star polymers synthesised by reversible-deactivation radical polymerization (also referred to as controlled radical polymerisation) via the arm-first approach have been studied in detail.[51] Synthesis of CCS polymers via the arm-first method allows for the precise pre-design of arm precursors and can thus lead to star polymers with well-defined structures and compositions. In our previous study, star polymers with a branched core (composed of ^{19}F-containing and pH-responsive units) and hydrophilic arms were prepared and utilised as

This journal is © The Royal Society of Chemistry [year]

selective ^{19}F MRI contrast agents with the potential for the detection of diseased tissues.[52] Although branched polymers bearing ^{19}F nuclei have been developed as ^{19}F MRI contrast agents, to the best of our knowledge, CCS polymers with fluorinated units in the arms have not been reported as ^{19}F MRI agents. In this paper we investigate the effect of placement of ^{19}F nuclei and pH-responsive units in the block copolymer arms instead of in the branched core.

In this paper, we aim to synthesise core crosslinked star (CCS) polymers as ^{19}F MRI contrast agents via the arm-first approach by reversible addition-fragmentation chain transfer (RAFT) polymerisation. As illustrated in Scheme 1, the arms are block copolymers that contain 2,2,2-trifluoroethyl methacrylate (TFEMA) units to provide ^{19}F NMR and MRI signal and 2-(dimethylamino)ethyl methacrylate (DMAEMA) segments to achieve pH-responsiveness. In addition, the cores are comprised of bis(2-methacryloyl)oxyethyl disulfide (DSDMA) crosslinked homopolymer, which is degradable in the presence of reducing agents. It is expected that the protonation and deprotonation of DMAEMA units in the copolymer arms in aqueous solution will not only influence the size of the nanoparticles but also alter the mobility of ^{19}F nuclei in the TFEMA segments, resulting in the variations in signal intensity and relaxation times of ^{19}F nuclei with pH. Moreover, selective imaging can be realised in ^{19}F MRI by utilising the pH-responsiveness of the ^{19}F relaxation times. Last but not least, since the CCS polymers have abundant disulfide bonds in the crosslinked core, the as-formed nanoparticles can be degraded by reducing agents such as dithiothreitol (DTT), tris(2-carboxyethyl)phosphine hydrochloride (TCEP) and glutathione (GSH),[53-55] and this biodegradability is especially desirable for future *in vivo* applications.

Experimental Section

Materials

All chemicals were purchased from Sigma-Aldrich unless otherwise stated. Poly(ethylene glycol) methyl ether methacrylate (PEGMA, *M*W = 475), 2-(dimethylamino)ethyl methacrylate (DMAEMA), 2,2,2-trifluoroethyl methacrylate (TFEMA), ethylene glycol dimethacrylate (EGDMA), butyl methacrylate (BMA) and 2-hydroxyethyl methacrylate (HEMA) were passed through basic alumina columns to remove inhibitors prior to use. The initiators, 2,2'-azobis(2-methylpropionitrile) (AIBN) and 4,4'-azobis(4-cyanovaleric acid) (ACVA) were recrystallised from ethanol twice before use. 4-Methoxyphenol (MEHQ), 4-(dimethylamino)pyridine (DMAP), triethylamine (TEA), N,N'-dicyclohexylcarbodiimide (DCC), tris(2-carboxyethyl)phosphine hydrochloride (TCEP) and L-glutathione reduced (GSH) were used as received. The trithiocarbonate RAFT agent, 4-cyano-4-(dodecylsulfanylthiocarbonyl)sulfanyl pentanoic acid (denoted as CTA), was synthesised following a previously reported method.[56] Milli-Q water with a resistivity of 18.4 MΩ.cm^{-1} was used for the synthesis and purification of polymers and preparation of aqueous solutions. Tetrahydrofuran (THF), dichloromethane (DCM) and toluene were obtained from a solvent purification system (SPS) and used directly.

Characterisation

Gel Permeation Chromatography (GPC) Molecular weights and molecular weight distributions were determined by GPC using a Waters Alliance 2690 Separations Module equipped with Waters 2414 Refractive Index (RI) Detector, Waters 2489 UV/Visible Detector, Waters 717 Plus Autosampler and Waters 1515 Isocratic HPLC Pump. Samples were dissolved in THF/triethylamine (95/5, v/v) and passed through 0.45 μm filters before each measurement. THF was used as the mobile phase at a flow rate of 1 mL/min. The system was calibrated using polystyrene (PS) standards, to which the number average molecular weight (M_n) and weight average molecular weight (M_w) were referenced. Absolute molecular weights of the star polymers were measured by a triple detection GPC (Polymer Labs GPC50) equipped with dual angle laser light scattering detector, viscometer and differential refractive index detector. N,N-dimethylacetamide (DMAc, HPLC grade, containing 0.03 wt % LiCl) was used as the eluent at a flow rate of 1.0 mL min^{-1}. Separations were achieved using two PLGel Mixed B (7.8 × 300 mm) columns connected in series and held at a constant temperature of 50 °C. The triple detection system was calibrated using a 2 mg mL^{-1} PSTY standard (Polymer Laboratories, Mw = 110 K, dn/dc = 0.16 mL g^{-1} and IV = 0.5809). Samples of given concentrations were prepared in DMAc (containing 0.03 wt% LiCl) and passed through a 0.45 μm PTFE syringe filters prior to measurements. The absolute molecular weights and dn/dc values were determined by using Polymer Laboratories Multi Cirrus software based on the quantitative mass recovery technique.

Nuclear Magnetic Resonance (NMR) ^{1}H NMR and ^{13}C NMR analysis were performed on a Bruker Avance 500 MHz spectrometer equipped with a BBO5 probe at 25 °C using an internal lock ($CDCl_3$) and referenced to the residual non-deuterated solvent ($CHCl_3$).

Dynamic Light Scattering (DLS) DLS measurements were carried out on a Nanoseries Zetasizer (Malvern, UK) at 25 °C. Sample solutions were prepared in PBS (1 mg/mL) at different pH values and passed through 0.45 μm filters prior to each measurement. Each hydrodynamic diameter was the average value of 5 runs. To minimise the influence of large aggregates, number averaged diameters are reported.

^{19}F Nuclear Magnetic Resonance (^{19}F NMR) All ^{19}F NMR spectra were acquired at 470.55 MHz without ^{1}H decoupling on a Bruker Avance 500 spectrometer using a 5 mm broadband inverse probe (BBO5) for which the inner coil was double-tuned for ^{19}F and ^{1}H. The samples were prepared by dissolving the star polymers in PBS/D_2O (90/10, v/v) at a concentration of 20 mg/mL. All measurements were performed at 25 °C. A 90° pulse of 15.1 μs was used in all measurements, the relaxation delay was 2 s and the acquisition time was 0.7 s. Data were collected using a spectrum width of 23 kHz, 32k data points and 128 scans.

^{19}F spin-spin relaxation times (T_2) were measured using the Carr-Purcell-Meiboom-Gill (CPMG) pulse sequence at 25 °C. The samples were dissolved in PBS/D_2O (90/10, v/v) at a concentration of 20 mg/mL. The relaxation delay was 3 s and the acquisition time was 0.7 s. For each measurement, the echo times were from 2 to 770 ms and 15 points were collected, which could be described by exponential functions for the calculation of T_2.

^{19}F spin-lattice (T_1) relaxation times were measured using the standard inversion-recovery pulse sequence. For each

measurement, the recovery times were from 2 ms to 3 s and 15 points were acquired. Values for the major peak at around -72.6 ppm are reported.

^{19}F Magnetic Resonance imaging (^{19}F MRI)

Images of phantoms containing the solutions of the CSS particles were acquired on a Bruker BioSpec 94/30 USR 9.4 T small animal MRI scanner. CCS polymers were dissolved in PBS/D_2O (90/10,v/v) to a concentration of 20 mg/mL and placed in a ^{1}H/^{19}F dual resonator 40 mm volume coil. ^{1}H were acquired for localisation of the samples using a RARE sequence with an echo train length of 8 (TE = 28 ms, TR = 2 s, FOV = 40 × 40 × 1 mm, Matrix = 128 × 128 × 1). ^{19}F images were acquired in the same stereotactic space as the ^{1}H image using a RARE sequence with an echo train length of 8 (TE = 10 ms, effective TE = 40 ms, TR = 1 s, FOV = 40 × 40 × 30 mm, Matrix = 32 × 32 × 1) with a total acquisition time of 1 hour 8 minutes.

Synthesis of alkyne-terminated chain transfer agent (alkyne-CTA)

The CTA (4.04 g, 10 mmol), propargyl alcohol (1.46 mL, 25 mmol) and DMAP (0.24 g, 2 mmol) were dissolved in 130 mL of DCM in a 250 mL flask, which was sealed with a rubber septum and then bubbled with argon for 30 min in an ice bath. Following this, DCC (4.13 g, 20 mmol) in 20 mL of DCM was injected dropwise into the flask. The reaction was kept in the ice bath and magnetically stirred for 2 h, followed by stirring at room temperature for 48 h. After the reaction, the mixture was filtered to remove the insoluble dicyclohexylurea precipitate. The filtrate was washed with water (100 mL × 2) and brine (100 mL × 2), and then dried over anhydrous $MgSO_4$. Finally, the solvent was removed by rotary evaporation, and the residual oil was further purified by flash column chromatography (SiO_2, gradient petroleum spirit/ethyl acetate, from 9/1 to 8/2), yielding a scarlet oil (3.7 g, 84% yield).

^{1}H NMR (500 MHz, δ, ppm, $CDCl_3$): 0.88 (t, 3H, CH_3CH$_2$CH$_2$), 1.26 (br s, 18H, (CH$_2$)$_9$), 1.69 (m, 2H, CH_2CH$_2$S), 1.87 (s, 3H, CH_3), 2.37-2.70 (m, 4H, CH$_2$CH$_2$-COO), 2.49 (t, H, OCH$_2$C≡CH), 3.32 (t, 3H, CH$_2$CH_2S), 4.70 (d, 2H, OCH_2C≡CH).

^{13}C NMR (125 MHz, δ, ppm, $CDCl_3$): 170.63 (*C*OOCH$_2$), 118.87 (*C*N), 75.20 (*C*≡CH), 52.41(C≡*C*H), 46.21 (*C*(CH$_3$)CN)), 37.03 (C(=O)CH$_2$*C*H$_2$), 33.62 (C(=O)*C*H$_2$CH$_2$), 31.85, 29.56, 27.61, 24.81, 22.63 (overlapping ^{13}C signals), 14.07 (*C*H$_3$CH$_2$CH$_2$).

Synthesis of poly PPEGMA macro-CTA

PEGMA (24 g, 50 mmol), alkyne-CTA (0.886 g, 2 mmol), AIBN (66 mg, 0.4 mmol) were dissolved in 50 mL of toluene in a 100 mL flask, which was sealed with a rubber septum and bubbled with argon for 1 h in an ice bath. Then the flask was immersed in an oil bath maintained at 70 °C and magnetically stirred. At given intervals, samples were withdrawn using a gas-tight syringe for measurement of extent of conversion. After 180 min, the polymerisation was quenched by cooling the flask in an ice bath and exposing the solution to air. The crude solution was precipitated into cold hexane 3 times and then dialysed against water for 2 days. After lyophilisation, a yellow oil was obtained. Yield: 11 g, 94%). GPC: M_n = 7200, molar mass dispersity ($Đ_M$, M_w/M_n) = 1.12. ^{1}H NMR: DP = 14, M_n = 7100.

Synthesis of PPEGMA-b-P(TFEMA-co-DMAEMA) block copolymers

In a typical experiment, the macro-CTA (0.665 g, 0.094 mmol), TFEMA (0.144 mL, 1 mmol), DMAEMA (0.674 mL, 4 mmol) and AIBN (3.3 mg, 0.02 mmol) were dissolved in 4 mL of toluene. The solution was equally divided into 5 tubes, each of which was purged with nitrogen for 5 min in an ice bath before being placed in a 70 °C oil bath. The tubes were opened and cooled to 0 °C at various time intervals to allow measurement of conversion.

For the fully scaled-up synthesis, the macro-CTA (3.6 g, 0.51 mmol), TFEMA (0.771 mL, 5.4 mmol), DMAEMA (3.649 mL, 21.6 mmol) and AIBN (17.8 mg, 0.102 mmol) were dissolved in 22 mL of toluene in a 100 mL flask, which was sealed with a rubber septum and purged with nitrogen for 30 min in an ice bath. The flask was placed in a 70 °C oil bath for 2.5 h, followed by being cooled to 0 °C and exposed to air. The sample was purified by precipitation into cold hexane 3 times and dried under vacuum. A yellowish viscous solid was obtained. Yield: 4.86 g, 86%. The degree of polymerisation (DP) was calculated from ^{1}H NMR, and the composition of the block copolymer was confirmed to be PPEGMA$_{14}$-b-(TFEMA$_5$-co-DMAEMA$_{19}$) (10500 by ^{1}H NMR), $Đ_M$= 1.21 (by GPC).

Synthesis of CCS polymers using EGDMA as crosslinker

CCS polymers were synthesised by the arm-first approach through dispersion polymerisation. Typically, PPEGMA$_{14}$-b-(TFEMA$_5$-co-DMAEMA$_{19}$) (0.210 g, 0.02 mmol), BMA (16 µL, 0.1 mmol), EGDMA (20 mg, 0.1 mmol) and ACVA (1.12 mg, 0.004 mmol) were added to a mixture of 2 mL ethanol and 2 mL water. The solution was stirred at room temperature for 30 min to form a clear solution, before being divided into 5 tubes containing stirrer bars. Each tube was sealed with a rubber septum, followed by being purged with nitrogen for 15 min in an ice bath. After that, the tubes were immersed in 70 °C oil bath, and were opened at given time intervals for GPC and DLS analysis.

Synthesis of bis(2-methacryloyl)oxyethyl disulfide (DSDMA)

Degradable crosslinker DSDMA was synthesised using a published procedure,[57] with minor modification. 2-Hydroxyethyl disulfide (7.7 g, 0.05 mol) and MEHQ (60 mg) were added to 150 mL DCM in a 500 mL flask, and a heterogeneous mixture was formed. Then methacryloyl chloride (20 mL, 0.2 mol) was added to the mixture. The flask was immersed in an ice/water bath and TEA was added drop-wise using a dropping funnel over 40 min. During addition of the TEA, a white precipitate was gradually formed. After the addition of TEA, the mixture was stirred at 0 °C for another 30 min and then at room temperature for 24 h. After reaction, the mixture was filtered to remove the the insoluble triethylamine hydrochloride salt. Then the filtrate was washed with 1 M $NaHCO_3$ solution (150 mL × 3) and water (150 mL × 3), and the organic phase was dried over anhydrous $MgSO_4$ with 60 mg of MEHQ. After that, DCM was removed by rotary evaporation. The residual was purified by flash column chromatography (SiO_2, gradient hexane/ethyl acetate, from 90/10 to 60/40). A slightly yellowish oil was obtained and was stored in a freezer in dark. Yield: 8.9 g, 61%.

This journal is © The Royal Society of Chemistry [year]

Synthesis of biodegradable CCS polymers using DSDMA as crosslinker

$PPEGMA_{14}$-b-($TFEMA_6$-co-$DMAEMA_{20}$) (0.216 g, 0.02 mmol), DSDMA (58 mg, 0.2 mmol) and ACVA (2.24 mg, 0.005 mmol) were added to a mixture of 2 mL ethanol and 2 mL water, which was then stirred at room temperature for 30 min to form a clear solution. After that the solution was divided equally to 4 tubes, and each tube was purged with nitrogen for 10 min in an ice bath. Finally the tubes were placed in a 70 °C oil bath, and each tube was opened and cooled to 0 °C periodically. GPC measurements were carried out for each sample to monitor the formation of CCS polymer.

For the scale-up synthesis, $PPEGMA_{14}$-b-($TFEMA_6$-co-$DMAEMA_{20}$) (2.16 g, 0.2 mmol), DSDMA (0.58 g, 2 mmol) and ACVA (22.4 mg, 0.05 mmol) were added to a mixture of 20 mL ethanol and 20 mL water in a 100 mL flask, which was then sealed with a rubber septum and purged with nitrogen for 45 in an ice bath. Then the flask was immersed in 70 °C oil bath for 30 min. After polymerisation, the sample was purified using centrifugal filter units (Amicon Ultra-15, 100k) and then lyophilised.

Degradation of star polymer by reduction with TCEP

SP-1 (30 mg, 4.6×10^{-5} mmol) was dissolved in 6 mL of methanol in a 20 mL schlenk tube, which was then magnetically stirred and purged with Ar. After 30 min, TCEP (86 mg, 0.3 mmol) was added to the polymer solution under the protection of Ar. The solution was stirred at RT for 7 hours, followed by the injection of pre-deoxygenated TEA (100 µL, 0.72 mmol) and MMA (200 µL, 1.87 mmol) to cap the formed thiol groups. After stirring at RT overnight, the reaction was stopped through exposure to air and an aliquot was withdrawn for GPC analysis.

Degradation of star polymer by reduction with GSH

SP-1 (15 mg, 2.3×10^{-5} mmol) was dissolved in 30 mL of PBS in a 100 mL flask and the pH was adjusted to 7.4 using 1 M NaOH solution. The flask was then sealed with a rubber septum and purged with Ar for 30 min, followed by the addition of GSH (92 mg, 0.3 mmol) under Ar flow. The solution was purged with Ar for another 30 min and stirred at 37 °C. After 72 h, pre deoxygenated TEA (200 µL, 1.44 mmol) and HEMA (250 µL, 2.06 mmol) were injected to the flask to cap the thiol groups that were formed after reduction. After another 24 h the sample was freeze dried and subjected to GPC analysis.

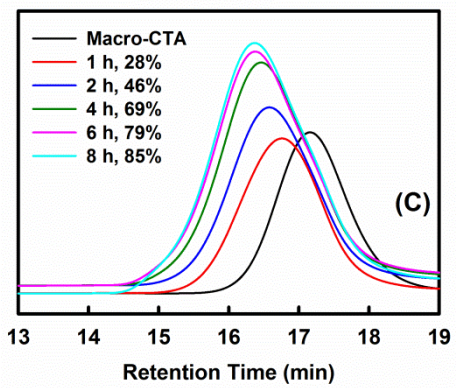

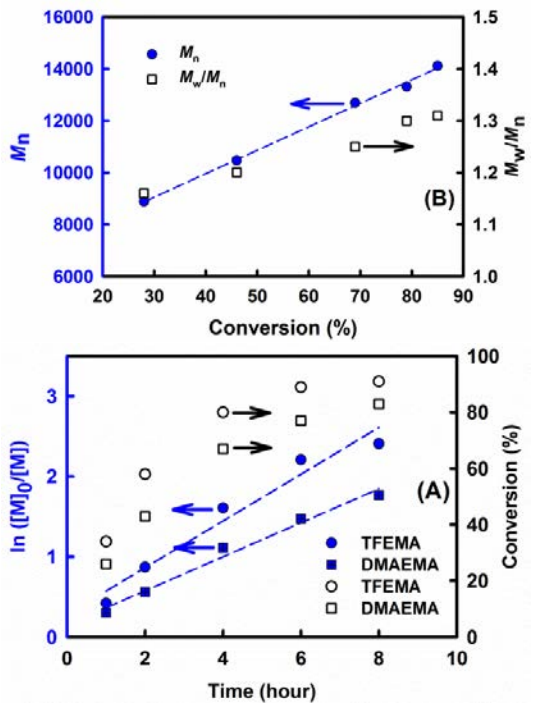

Fig. 1 RAFT polymerisation of TFEMA and DMAEMA using PPEGMA macro-CTA. (A) Pseudo-first-order kinetic plots of the polymerisation. (B) Dependence of number-average molecular weight (M_n, determined by GPC) and molar-mass dispersity ($Đ_M$) on the total monomer conversion. (C) GPC traces during the polymerisation.

Table 1 Properties of the macro-CTA and arm precursors.

Sample	^{19}F[a] wt%	M_n[b] (GPC)	$Đ_M$[b]	M_n[c] (^{1}H NMR)
Macro-CTA ($PPEGMA_{14}$)	-	7200	1.12	7100
Arm-1 ($PPEGMA_{14}$-*b*-($TFEMA_5$-*co*-$DMAEMA_{19}$)	3.2	9200	1.24	10500
Arm-2 ($PPEGMA_{14}$-b-($TFEMA_{11}$-co-$DMAEMA_{15}$)	5.5	8900	1.20	11300
Arm-3 ($PPEGMA_{14}$-b-($TFEMA_{18}$-co-$DMAEMA_{10}$)	8.8	8900	1.18	11700

[a] Weight percentage of fluorine in the samples. [b] M_n and $Đ_M$ acquired by GPC RI detector. [c] M_n calculated using the DP given by ^{1}H NMR.

Results and Discussion

Synthesis of PPEGMA macro-CTA

A trithiocarbonate chain transfer agent, 4-cyano-4-(dodecylsulfanylthiocarbonyl)sulfanyl pentanoic acid, was first end functionalised with propargyl alcohol and subsequently used for the synthesis of PPEGMA macro-CTA, as reported in our previous study.[52] The alkyne end group can offer the possibility of further modification of the CCS polymer through 'click'

chemistry. Furthermore, the alkyne end group facilitates the calculation of the degree of polymerisation (DP) using ^{1}H NMR owing to the well-resolved peak (~4.7 ppm) due to the protons in the methylene group adjacent to the alkyne group. PEGMA was chosen because of its hydrophilicity and biocompatibility. The kinetics of the synthesis of PPEGMA was investigated, and the results confirmed a well-controlled RAFT polymerisation (Fig. S1, ESI†). The PPEGMA so-formed (DP = 14, M_n (^{1}H NMR) = 7100, $Đ_M$ = 1.12) was used as the macro-CTA in subsequent steps.

Synthesis of PPEGMA-b-P(TFEMA-co-DMAEMA) block copolymers

The as-synthesised PPEGMA macro-CTA was chain extended with TFEMA and DMAEMA for the synthesis of PPEGMA-b-P(TFEMA-co-DMAEMA). As displayed in Fig. 1, the polymerisation rates of both TFEMA and DMAEMA exhibited pseudo-first-order kinetics throughout the polymerisation to above 80% conversion (Fig. 1 (A)). In addition, the number-average molecular weight increased linearly with monomer conversion while the molar-mass dispersity ($Đ_M$) remained relatively low (Fig. 1 (B)). Furthermore, the GPC curves also evolved from long retention time to short retention time with increase of reaction time and conversion (Fig. 1 (C)). This confirms the successful synthesis of PPEGMA-b-P(TFEMA-co-DMAEMA) from the PPEGMA macro-CTA. To minimise the loss of trithiocarbonate end group, a monomer conversion of ~50% was targeted in the scale-up polymerisation. After purification, PPEGMA$_{14}$-b-(TFEMA$_5$-co-DMAEMA$_{19}$) was obtained (denoted as Arm-1, M_n = 10500 by ^{1}H NMR, $Đ_M$ = 1.21). In order to prepare block copolymers with different compositions, Arm-2 (PPEGMA$_{14}$-b-(TFEMA$_{11}$-co-DMAEMA$_{15}$, M_n = 11300 by ^{1}H NMR, $Đ_M$ = 1.20) and Arm-3 (PPEGMA$_{14}$-b-(TFEMA$_{18}$-co-DMAEMA$_{10}$, M_n = 11700 by ^{1}H NMR, $Đ_M$ = 1.18) were then synthesised by adjusting the TFEMA/DMAEMA ratio and using the same polymerisation condition. The properties of the macro-CTA and block copolymers are summarised in Table 1.

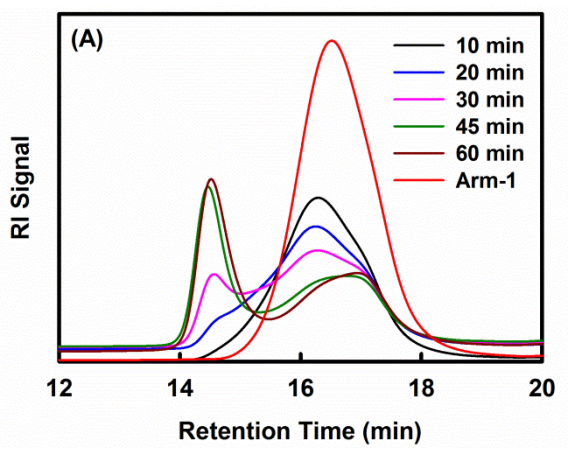

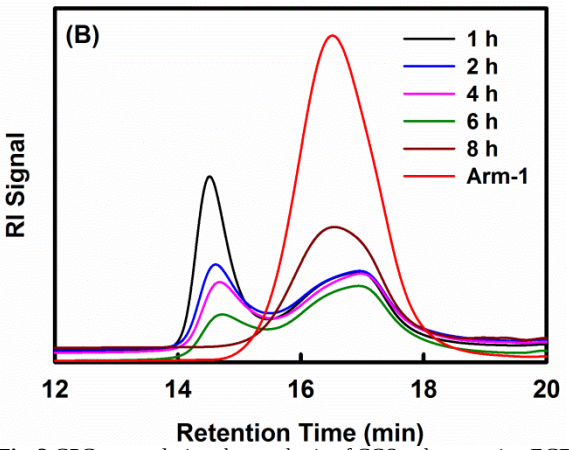

Fig. 2 GPC traces during the synthesis of CCS polymer using EGDMA as crosslinker by dispersion polymerisation. Condition: [Arm-1]/[BMA]/[EGDMA]/[ACVA] = 1/5/5/0.2, [arm-1] = 5 mM, in water/ethanol (50/50, v/v), 70 °C.

Synthesis of CCS polymers through RAFT dispersion polymerisation by the arm-first approach

Recently, RAFT dispersion polymerisation has been exploited for the synthesis of CCS polymers by the An group and its benefits have been discussed and highlighted.[58-61] Compared to conventional homogeneous polymerisation in organic solvents, the heterogeneous polymerisation in aqueous solution can significantly reduce the polymerisation time due to an accelerated monomer consumption. Furthermore, the method can increase the yield of star polymer by facilitating the arm incorporation process. As the three block copolymers were all water soluble due to the hydrophilic PPEGMA segments, RAFT dispersion polymerisation in water/ethanol mixture was introduced for the synthesis of CCS polymers.

The CCS polymers were synthesised through the chain extension of arm precursors with the crosslinker EGDMA. The polymerisation was carried out in water/ethanol mixture (50/50, v/v) at 70 °C using ACVA as initiator. It was found that the polymerisation time played a pivotal role in the formation of CCS polymers. Fig. 2 shows the GPC traces of the samples withdrawn at different polymerisation times during the dispersion polymerisation. As one can see in Fig. 2 (A), although the peak in the traces due to the arms became broader and started to shift toward shorter retention times, no well-defined CCS polymer was formed within 20 min. After 30 min, a peak appeared at retention time of 14.6 min and could be assigned to the CCS polymer. Over the next 30 min the intensity of the CCS peak continued to rise while that of the linear polymer peak at 16.2~17.0 decreased gradually, indicating increasing arm incorporation and yield of CCS polymer. Interestingly, as shown in Fig. 2 (B), the intensity of the CCS polymer peak decreased by half after 2 hours, and then continued to be diminished over the next 4 hours before it completely disappeared after 8 hours.

Based on the GPC traces, the extent of formation of the CCS polymer through the chain extension of block copolymer with crosslinker reached a maximum after 1 hour. However, due to monomer consumption and abundant vinyl groups in the core, after 1 hour intermolecular coupling (or star-star coupling) started to dominate the polymerisation, and resulted in the formation of

This journal is © The Royal Society of Chemistry [year]

macroscopic gel particles, which consumed the as-formed CCS polymers and substantially reduced the CCS polymer yield. In support of this a digital photo of the samples at increasing conversion demonstrates a change from clear solution to turbid dispersion (Fig. S2, ESI†), confirming the gradual formation of larger, insoluble particles after 1 hour. Furthermore, the particle size (number averaged diameter) of the crude polymerisation solution increased significantly from 7.4 nm after 10 minutes to 13.4 nm after 1 hour, slowly increased to 14.8 nm after 6 hours before dramatically increasing to ~360 nm after 8 hours (Fig. S3, ESI†). After filtration, the particle size became smaller owing to the removal of large particles (Fig. S3, ESI†).

A number of other significant parameters in the polymerisation were also investigated. It was found that the water/ethanol ratio was a key factor since well-defined CCS polymer were only formed in water/ethanol (50/50, v/v) (Fig. S4 (A), ESI†). This is understandable since a higher ethanol content in the polymerisation solvent (> 75 %) will result in homogeneous polymerisation; CCS polymers usually take much longer to form (typically 8~24 h) in organic solvents[62-65] than dispersion polymerisation. However, the arm precursor has poor solubility when the ethanol content is too low (< 50 %). Therefore a moderate water/ethanol ratio is required for a successful dispersion polymerisation, so that the starting reagents dissolve well while the CCS polymer has poor solubility. In addition, unlike other reports,[59, 60, 62] the use of the spacing monomer did not improve the formation of CCS polymer. Moreover, the highest yield of CCS polymers was achieved when [EGDMA]/[arm-1] ratio was 10 or 15 (Fig. S4 (C), ESI†). As shown in ESI† Fig. S4 (D), the CCS polymer yield was also increased by using a higher [ACVA]/[Arm-1] ratio (2/5). These results revealed that the arm-first synthesis of CCS polymer via RAFT dispersion polymerisation could be affected by a number of parameters and well-defined CCS polymers with high yield could be obtained by carefully selecting and controlling the polymerisation conditions.

A degradable crosslinker, bis(2-methacryloyl)oxyethyl disulfide (DSDMA), was then chosen for the synthesis the CCS polymers. As displayed in Fig. 3 (A), well-defined CCS polymer can be synthesised within 30 min with the highest yield (74%). At longer reaction times star-star coupling became more important, as evidenced by the decrease in the peak in the GPC traces due to the CCS polymer. The as-synthesised CCS polymer (denoted as CCS-1) was purified using centrifugal filter units. In Fig. 3 (B), one can see that most of the linear residues were removed after purification (black line). The polymers in the filtrate (denoted as Filtrate-1) were also collected and examined by GPC and ^{1}H NMR. According to the GPC trace (green line), despite the presence of a small amount of CCS polymer (1.21%), the linear residues showed a smaller M_n compared to that of Arm-1while its $Đ_M$ was as low as that of Arm-1. In addition in the ^{1}H NMR, as shown in ESI† Fig. S5 (B), for Filtrate-1, the peak intensity of the protons of the CH_2 next to the trithiocarbonate considerably decreased compared with Arm-1, suggesting that the residual linear polymers had very low end group functionality. The structure of the residual polymer was confirmed to be PPEGMA$_{14}$-b-P(TFEMA$_3$-co-DMAEMA$_8$) by ^{1}H NMR with M_n of 8400. We therefore conclude that the residual linear polymer collected from the filtrate is block copolymer in which the trithiocarbonate end groups have been lost during the synthesis of the arm precursor.

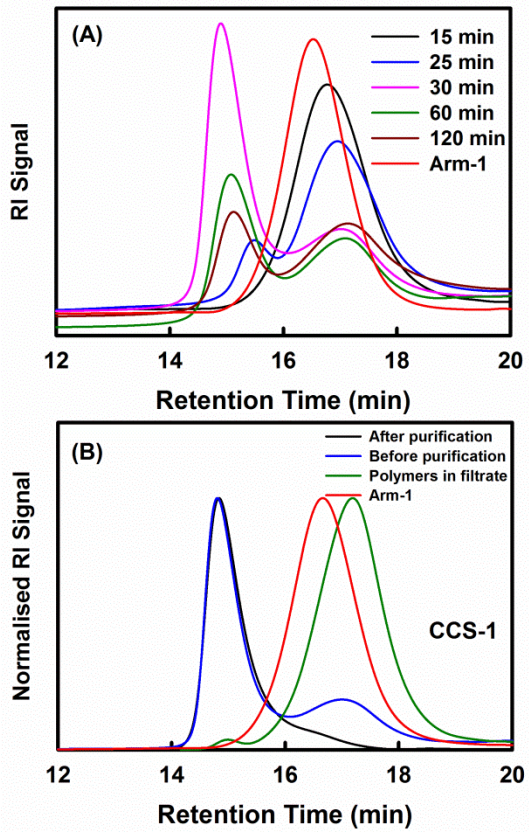

Fig. 3 GPC traces of CCS polymer synthesised using DSDMA as crosslinker. (A) GPC traces at different polymerisation time. (B) GPC traces of CCS polymer prepared after 30 min. Condition: [Arm-1]/[DSDMA]/[ACVA] = 1/10/0.4, [arm-1] = 5 mM, in water/ethanol (50/50, v/v), 70 °C.

In the ^{1}H NMR spectrum of CCS-1 (Fig. S5 (C), ESI†) peaks at 5.6 and 6 ppm were assigned to the unreacted vinyl groups that were likely to be in the periphery of the core. Nevertheless, the DSDMA units could not be fully detected due to the highly rigid nature of the core.[66] The ^{13}C NMR spectrum (Fig. S5 (D), ESI†) further confirmed the absence of a peak at ~222 ppm due to the trithiocarbonate carbons. It is well known that the increased dipolar couplings experienced in rigid cores of particles may prevent direct observation by solution-state NMR methods.

Table 2 Details of the CCS polymers.

Sample	^{19}F wt%	M_n (GPC)	$Đ_M$	Absolute MW	$Đ_M$	f
CCS-1	2.3	32800	1.23	653,300	1.17	46
CCS-2	3.9	43300	1.19	482,500	1.07	31
CCS-3	6.1	28000	1.19	683,000	1.15	41

[a] Fluorine content in the samples. [b] M_n and $Đ_M$ of crude CCS polymers given by GPC RI detector. [c] Absolute MW and $Đ_M$ measured by triple detection GPC. [d] Number of arms (see the calculation in ESI†)

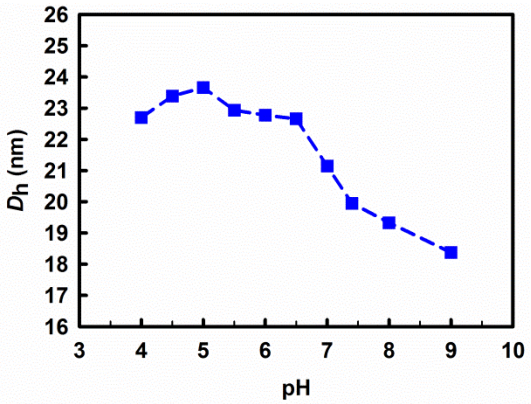

Fig. 4 Number averaged diameter of CCS-1 in PBS (1 mg/mL) at different pH at 25 °C.

A range of CSS polymers with different compositions were prepared by using Arm-2 and Arm-3 for the synthesis of CCS-2 and CCS-3, respectively, and the resulting CCS polymers were purified using the same procedure described above for CCS-1. The properties of the CCS polymers are listed in Table 2.

The particle sizes of CCS-1 in PBS and at a range of pH values from 4 to 9 were measured by DLS. As shown in Fig. 4, the particle size was around 23 nm when the pH was below 6.5 and decreased progressively with an increase in pH and finally reached ~18 nm at pH 9. The change in particle size arises from the DMAEMA units present in the arms; PDMAEMA is well known as a pH-responsive polymer and has a p*K*a between 7.3~7.5. Specifically, in aqueous solution, the protonation of the tertiary amines below p*K*a renders the PDMAEMA segments charged and the chains undergo electrostatic repulsion, while on deprotonation above p*K*a the chains adopt a more contracted configuration. On the basis of the DLS results, the volume of CCS-1 nanoparticles at pH 9 was reduced by 53% compared to that at pH 5, indicating a significant dependence of particle size on environmental pH.

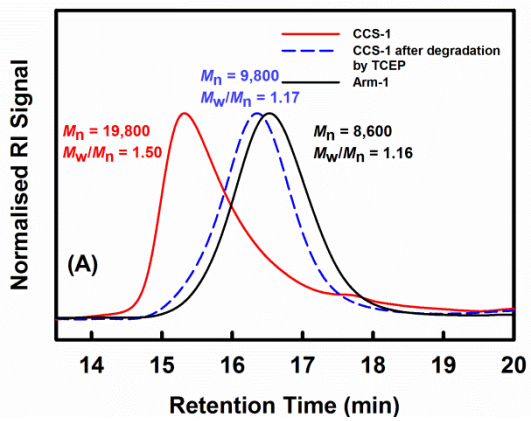

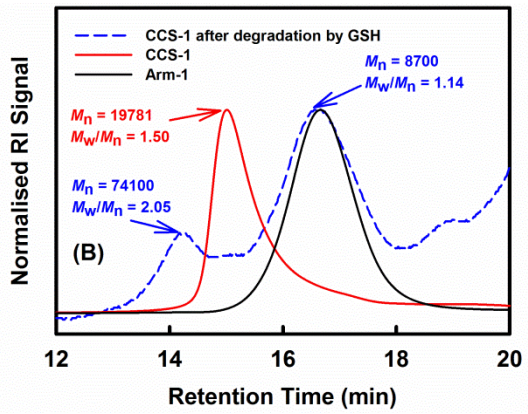

Fig. 5 GPC traces of CCS-1 before and after degradation by TCEP (A) and GSH (B), respectively

Degradation of CCS polymer

Disulfide-containing crosslinkers have been frequently used for the preparation of degradable materials because the disulfide group can be cleaved to thiols by reducing agents.[67] As the core of the as-synthesised CCS polymer is comprised of PDSDMA homopolymer, it is expected that the core can be degraded when treated with reducing agents. The degradation of CCS-1 in methanol was first tested using TCEP as the reducing agent, and the GPC curve shifted to longer retention time after 7 hours while the $Đ_M$ was as low as that of Arm-1 (Fig. 5 (A)), confirming the successful cleavage of the disulfide bonds in the core. It should be noted that the thiol groups in solution are very sensitive to oxygen and can form disulfide again when exposed to air. For example, after reduction of the CCS-1 with DTT in THF, samples were withdrawn periodically for GPC analysis, and the GPC curves of the degraded polymer shifted progressively to longer retention time and the $Đ_M$ became very large (39~98) owing to the re-formation of disulfide linkages in air (Fig. S7, ESI†). To avoid the re-formation of disulfides, after degradation the thiol groups were capped with MMA through based-catalysed Michael addition.[68, 69]

Since TCEP is not physiologically available, glutathione (GSH) was then chosen for the degradation of CCS-1. It has been reported that GSH is present in the human body at micromolar concentrations in blood plasma, ~10 mM in the cytosol [53, 70] and at several times higher concentration in tumour cells than normal cells.[71, 72] As shown in Fig. 5 (B), two peaks appeared after degradation with TCEP. To be more specific, the major peak with M_n of 8700 was from the linear polymers after the degradation of the crosslinked core, while the minor peak with M_n of 74100 was caused by the re-formation of disulfide groups due to the incomplete degradation of the core. As the core was comprised of hydrophobic PDSDMA that was poorly accessible for water and the GSH concentration was also relatively low, we propose that the degradation of CCS-1 using 10 mM GSH in PBS would take much longer time than the degradation by TCEP. Based on these results, we conclude that the as-synthesised CCS polymers were biodegradable.

This journal is © The Royal Society of Chemistry [year]

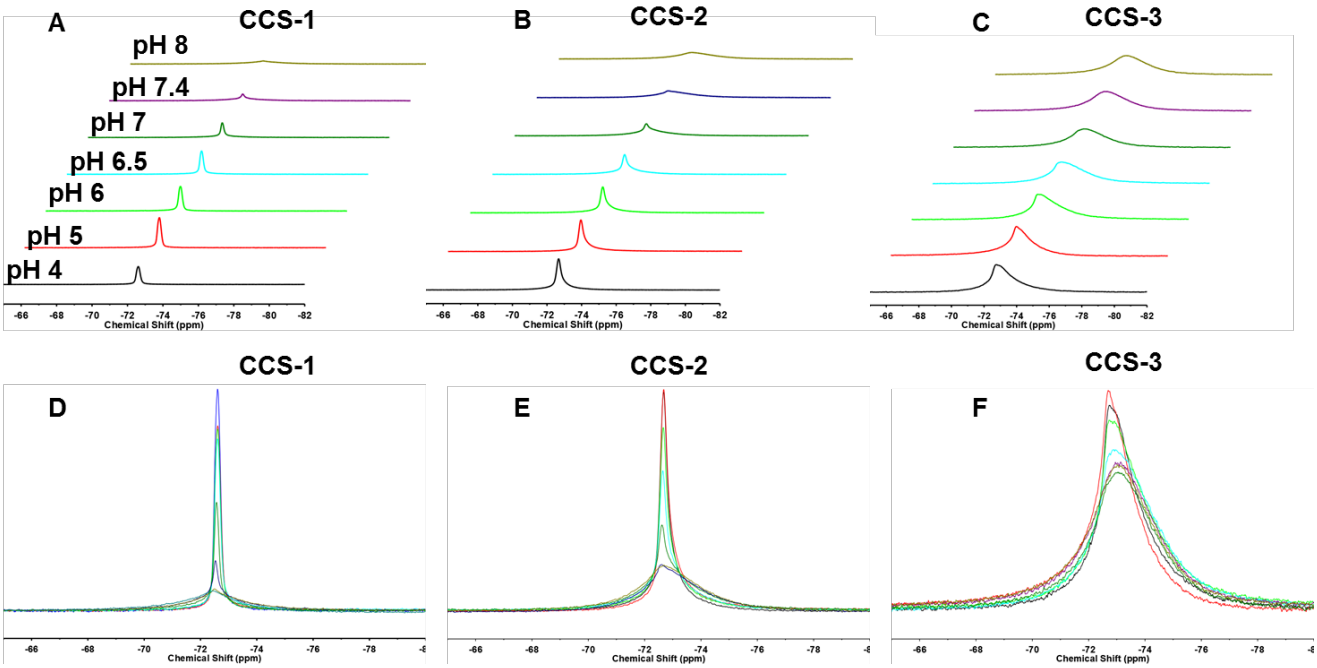

Fig. 6 ^{19}F NMR spectra of the CCS polymers in PBS/D2O (90/10, v/v) with 20 mg/mL concentration at 25 °C.

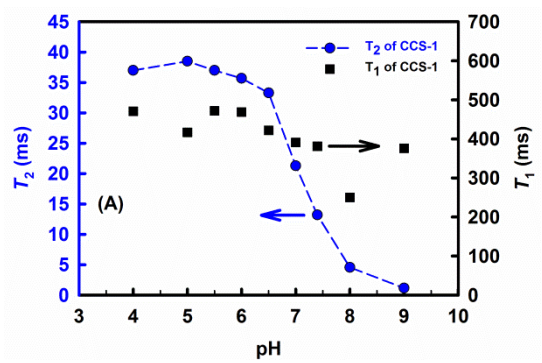

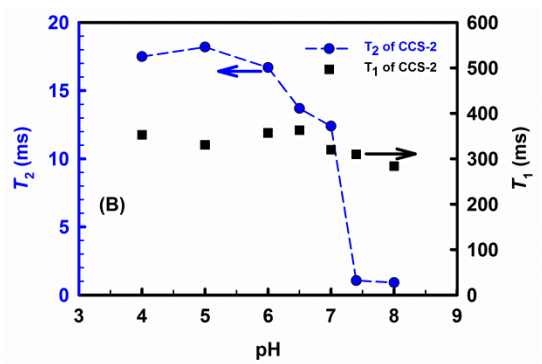

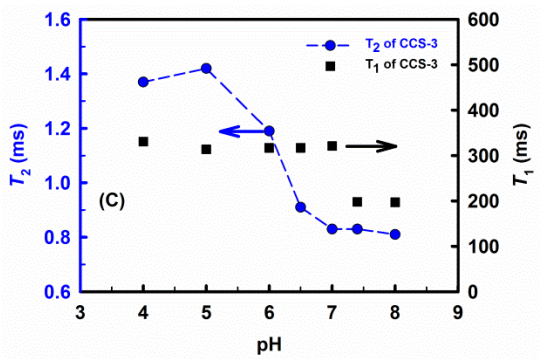

Fig. 7 Relaxation times of CCS-1 (A), CCS-2 (B) and CCS-3 (C) at different pH

^{19}F NMR study

In order to assess their potential as pH-responsive ^{19}F MRI contrast agents, the CCS polymers were examined by ^{19}F NMR in solutions with different values of pH. As displayed in Fig. 6, only one peak at -72.6 ppm was observed in each spectrum of all the three samples, confirming a single ^{19}F chemical environment in the CCS polymer structure. When the pH was raised, this peak became broader and the signal intensity decreased, as highlighted by the superimposed spectra in Fig. 6 (B), (D) and (F). As discussed above, the particle size was dependent on pH owing to the presence of the pH-sensitive monomer DMAEMA. An increase in pH leads to the deprotonation of PDMAEMA, thus the P(TFEMA-co-DMAEMA) block becomes hydrophobic and tends to aggregate in aqueous solution, reducing the mobility of ^{19}F nuclei. This leads to an increase in the NMR line width and a decrease in the ^{19}F signal intensity. In addition, it can be seen that the increase of ^{19}F content (from CCS-1 to CCS-3) also resulted

This is a post-print version of the following article: Wang, Kewei, Peng, Hui, Thurecht, Kristofer J., Puttick, Simon and Whittaker, Andrew K. (2014) Biodegradable core crosslinked star polymer nanoparticles as 19F MRI contrast agents for selective imaging. *Polymer Chemistry*, *5* 5: 1760-1771.

in a considerable decrease in the signal intensity because of the increased likelihood of association of the ^{19}F-containing segments. Overall, the ^{19}F NMR results indicated that the ^{19}F signal was dependent on both solution pH and ^{19}F content.

Spin-lattice (T_1) and spin-spin (T_2) relaxations times were also measured at different values of pH. For CCS-1, the T_2 first kept at around 35 ms below pH 6.5 and then dropped drastically to less than 5 ms at pH 8. The T_2 at pH 9 could not be measured due to the greatly attenuated signal. Meanwhile the T_1 was not greatly affected by the change of pH, indicating that the spectral density of high MHz motions of the fluoroethyl segments is not greatly affected by the change in polymer dimensions. Similar conclusions were reached by Peng *et al.* in their study of the behaviour of linear block copolymers.[23, 25] For CCS-2, the T_2 was much lower than that of CCS-1, but it showed a similar behaviour with changes in pH. As before, the T_2 above pH 7 could not be measured, demonstrating the reduced mobility of the ^{19}F nuclei. The T_2 of CCS-3 could not be measured at all values of pH owing to the self-association of ^{19}F-containing units and highly restricted motion, but was instead estimated from the width of the lines in the NMR spectra.

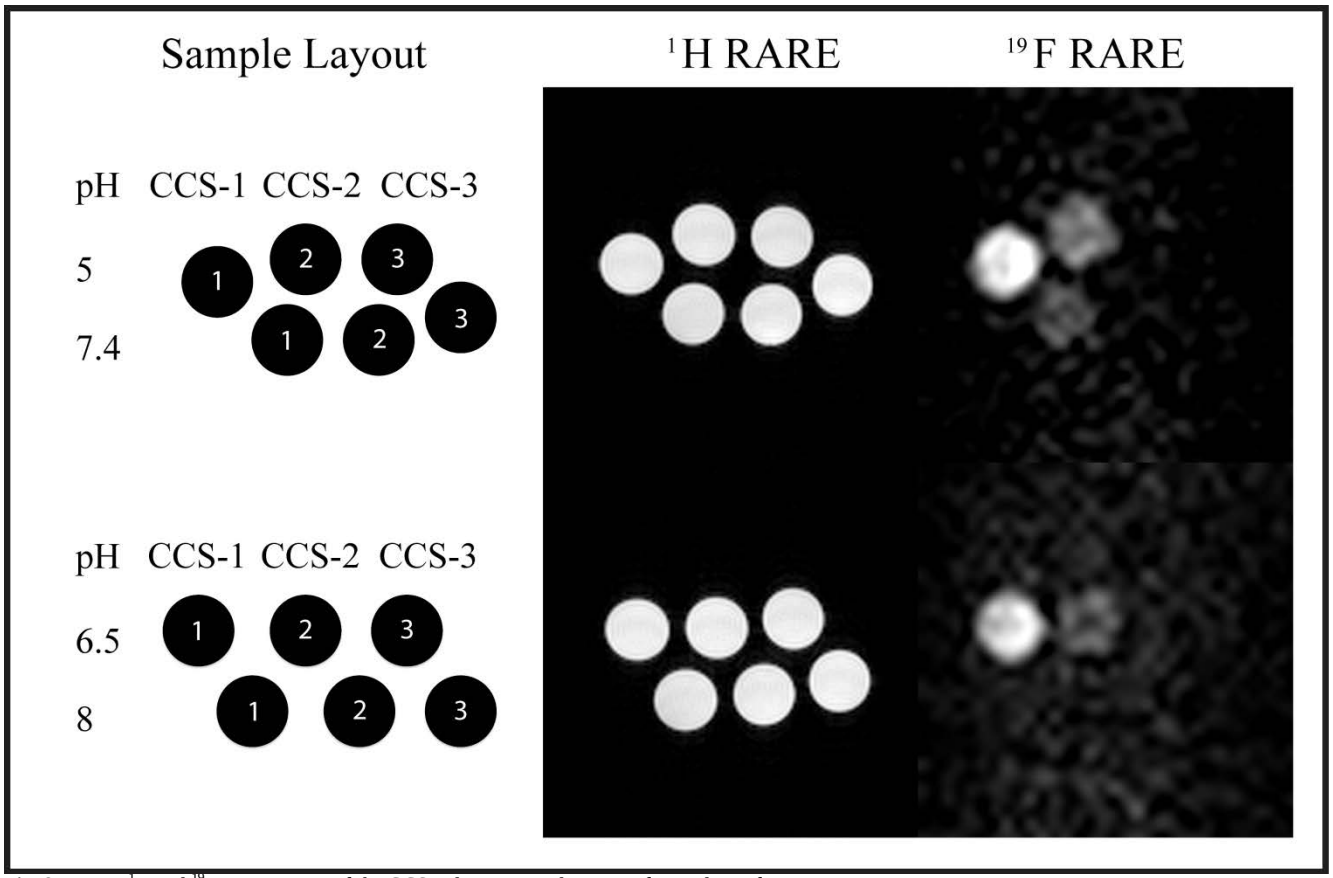

Fig. 8 In vitro ^{1}H and ^{19}F MRI images of the CCS polymers in solutions at four values of pH.

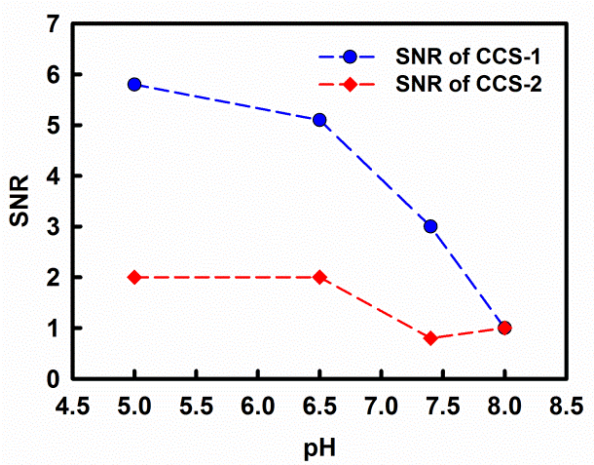

Fig. 9 Signal-to-noise ratio (SNR) of CCS-1 and CCS-2 at four pHs.

In vitro ^{19}F MRI evaluation

Following the ^{19}F NMR study, the CCS polymers were evaluated for in vitro ^{19}F MRI. As depicted in Fig. 8, ^{1}H RARE images were taken to allow localisation of the sample vials (phantoms). The ^{19}F MR images are shown on the right-hand side of Fig. 8. CCS-1 and CCS-2 showed a clear change in imaging performance at the four values of pH. Specifically, CCS-1 could be well visualised at pH 5, and the intensity decreased upon an increase of pH until being undetectable at pH 8. The figure demonstrates that CCS-2 was detected at pH 5 and 6.5 with poor signal-to-noise, and exhibited no signal at pH 7.4 and 8. Unsurprisingly, CCS-3 could not be imaged at all values of pH owing to its very short T_2 relaxation times. As shown in Fig. 9, a decrease in signal-to-noise ratio (SNR) was confirmed on an

This journal is © The Royal Society of Chemistry [year]

increase in pH of the polymer solution. On the basis of this ^{19}F MRI study, CCS-1 and CCS-2 showed better imaging performance at acidic pH. Thus it can be expected that these particles could be visualised only at acidic pH, and are thus potential candidates for the detection of tumour tissues that have acidic environments.

Our previous study of star polymers with fluorinated and DMAEMA units *within* the branched core also demonstrated a change in imaging performance with pH.[52] However, the best performing polymer in this current work (CCS-1) exhibited much better imaging performance at a comparable ^{19}F content. For this reason the MRI scan time could be notably shortened to 1 hour 8 minutes from 9 hours 6 minutes. We hypothesise that this improvement is attributed to the greater flexibility of polymer chains around the core for the CCS polymer compared with the segments within the relatively confined core-crosslinked structure.

Conclusions

In conclusion, CCS polymers were synthesised by RAFT dispersion polymerisation through the arm-first approach. The synthetic conditions were studied and optimised. The as-synthesised CCS polymer could form nanoparticles in aqueous solution and the particle size was dependent on pH. In addition, the CCS polymers were degradable due to the abundant disulfide bonds in the core. Moreover, ^{19}F NMR confirmed that the ^{19}F signal intensity was attenuated as the T_2 relaxation time decreased upon an increase of pH of the polymer solution. In vitro ^{19}F MRI indicated that the CCS polymers could be imaged well at acidic pH while they had poor imaging performance above physiological pH, demonstrating that these CCS polymers are promising ^{19}F MRI contrast agents for the selective imaging of tumour tissues.

Acknowledgements

The authors would like to acknowledge the Australian Research Council (DP0987407, DP110104299, LE0775684 and LE0668517) for funding and Australian National Fabrication Facility, Queensland Node for access to equipment. The authors would also like to thank Ms. Lynette Lambert at the Centre for Advanced Imaging, The University of Queensland for NMR assistance.

Notes and references

1. J. C. Knight, P. G. Edwards and S. J. Paisey, *Rsc Adv*, 2011, **1**, 1415-1425.
2. Z. X. Zhou and Z. R. Lu, *Wires Nanomed Nanobi*, 2013, **5**, 1-18.
3. Y. J. Liu and N. Zhang, *Biomaterials*, 2012, **33**, 5363-5375.
4. A. M. Mohs and Z. R. Lu, *Expert Opin Drug Del*, 2007, **4**, 149-164.
5. Z. R. Stephen, F. M. Kievit and M. Q. Zhang, *Mater Today*, 2011, **14**, 330-338.
6. A. K. Gupta and M. Gupta, *Biomaterials*, 2005, **26**, 3995-4021.
7. D. P. J. Pan, S. D. Caruthers, A. Senpan, A. H. Schmieder, S. A. Wickline and G. M. Lanza, *Wires Nanomed Nanobi*, 2011, **3**, 162-173.
8. M. F. Bellin, *Eur J Radiol*, 2006, **60**, 314-323.
9. A. P. Koretsky and A. C. Silva, *Nmr Biomed*, 2004, **17**, 527-531.
10. I. Aoki, S. Naruse and C. Tanaka, *Nmr Biomed*, 2004, **17**, 569-580.
11. H. J. Weinmann, W. Ebert, B. Misselwitz and H. Schmitt-Willich, *Eur J Radiol*, 2003, **46**, 33-44.
12. M. Bottrill, L. K. Nicholas and N. J. Long, *Chem Soc Rev*, 2006, **35**, 557-571.
13. D. D. Castelli, E. Gianolio, S. G. Crich, E. Terreno and S. Aime, *Coordin Chem Rev*, 2008, **252**, 2424-2443.
14. G. N. Holland, P. A. Bottomley and W. S. Hinshaw, *J Magn Reson*, 1977, **28**, 133-136.
15. J. Ruiz-Cabello, B. P. Barnett, P. A. Bottomley and J. W. M. Bulte, *Nmr Biomed*, 2011, **24**, 114-129.
16. J. X. Yu, V. D. Kodibagkar, W. N. Cui and R. P. Mason, *Curr Med Chem*, 2005, **12**, 819-848.
17. J. M. Janjic and E. T. Ahrens, *Wires Nanomed Nanobi*, 2009, **1**, 492-501.
18. S. Temme, F. Bonner, J. Schrader and U. Flogel, *Wires Nanomed Nanobi*, 2012, **4**, 329-343.
19. W. Liu and J. A. Frank, *Eur J Radiol*, 2009, **70**, 258-264.
20. M. M. Kaneda, S. Caruthers, G. M. Lanza and S. A. Wickline, *Ann Biomed Eng*, 2009, **37**, 1922-1933.
21. Y. Nose, *Artif Organs*, 2004, **28**, 807-812.
22. Z. X. Jiang, X. Liu, E. K. Jeong and Y. B. Yu, *Angew Chem Int Edit*, 2009, **48**, 4755-4758.
23. H. Peng, K. J. Thurecht, I. Blakey, E. Taran and A. K. Whittaker, *Macromolecules*, 2012, **45**, 8681-8690.
24. L. Nurmi, H. Peng, J. Seppala, D. M. Haddleton, I. Blakey and A. K. Whittaker, *Polym Chem-Uk*, 2010, **1**, 1039-1047.
25. H. Peng, I. Blakey, B. Dargaville, F. Rasoul, S. Rose and A. K. Whittaker, *Biomacromolecules*, 2009, **10**, 374-381.
26. M. M. Bailey, C. M. Mahoney, K. E. Dempah, J. M. Davis, M. L. Becker, S. Khondee, E. J. Munson and C. Berkland, *Macromol Rapid Comm*, 2010, **31**, 87-92.
27. S. Rossi, M. Benaglia, M. Ortenzi, E. Micotti, C. Perego and M. G. De Simoni, *Tetrahedron Lett*, 2011, **52**, 6581-6583.
28. M. M. Bailey, S. R. Kline, M. D. Anderson, J. L. Staymates and C. Berkland, *J Appl Polym Sci*, 2012, **126**, 1218-1227.
29. W. J. Du, A. M. Nystrom, L. Zhang, K. T. Powell, Y. L. Li, C. Cheng, S. A. Wickline and K. L. Wooley, *Biomacromolecules*, 2008, **9**, 2826-2833.
30. K. J. Thurecht, I. Blakey, H. Peng, O. Squires, S. Hsu, C. Alexander and A. K. Whittaker, *J Am Chem Soc*, 2010, **132**, 5336-5337.
31. M. Ogawa, H. Kataoka, S. Nitahara, H. Fujimoto, H. Aoki, S. Ito, M. Narazaki and T. Matsuda, *B Chem Soc Jpn*, 2012, **85**, 79-86.
32. M. Ogawa, S. Nitahara, H. Aoki, S. Ito, M. Narazaki and T. Matsuda, *Macromol Chem Phys*, 2010, **211**, 1602-1609.
33. M. Ogawa, S. Nitahara, H. Aoki, S. Ito, M. Narazaki and T. Matsuda, *Macromol Chem Phys*, 2010, **211**, 1369-1376.
34. J. M. Criscione, B. L. Le, E. Stern, M. Brennan, C. Rahner, X. Papademetris and T. M. Fahmy, *Biomaterials*, 2009, **30**, 3946-3955.
35. M. Oishi, S. Sumitani and Y. Nagasaki, *Bioconjugate Chem*, 2007, **18**, 1379-1382.
36. L. Josephson, M. F. Kircher, U. Mahmood, Y. Tang and R. Weissleder, *Bioconjugate Chem*, 2002, **13**, 554-560.
37. R. N. Muller, L. Vander Elst and S. Laurent, *J Am Chem Soc*, 2003, **125**, 8405-8407.
38. Y. T. Chang, C. M. Cheng, Y. Z. Su, W. T. Lee, J. S. Hsu, G. C. Liu, T. L. Cheng and Y. M. Wang, *Bioconjugate Chem*, 2007, **18**, 1716-1727.
39. M. F. Bennewitz, T. L. Lobo, M. K. Nkansah, G. Ulas, G. W. Brudvig and E. M. Shapiro, *Acs Nano*, 2011, **5**, 3438-3446.
40. G. L. Liang, J. Ronald, Y. X. Chen, D. J. Ye, P. Pandit, M. L. Ma, B. Rutt and J. H. Rao, *Angew Chem Int Edit*, 2011, **50**, 6283-6286.
41. D. Patel, A. Kell, B. Simard, B. Xiang, H. Y. Lin and G. H. Tian, *Biomaterials*, 2011, **32**, 1167-1176.
42. Y. Li, Y. Qian, T. Liu, G. Zhang and S. Liu, *Biomacromolecules*, 2012, **13**, 3877-3886.
43. B. A. Webb, M. Chimenti, M. P. Jacobson and D. L. Barber, *Nat Rev Cancer*, 2011, **11**, 671-677.
44. G. B. Giovenzana, R. Negri, G. A. Rolla and L. Tei, *Eur J Inorg Chem*, 2012, 2035-2039.

45. Y. Chen, Q. Yin, X. F. Ji, S. J. Zhang, H. R. Chen, Y. Y. Zheng, Y. Sun, H. Y. Qu, Z. Wang, Y. P. Li, X. Wang, K. Zhang, L. L. Zhang and J. L. Shi, *Biomaterials*, 2012, **33**, 7126-7137.
46. G. H. Gao, G. H. Im, M. S. Kim, J. W. Lee, J. Yang, H. Jeon, J. H. Lee and D. S. Lee, *Small*, 2010, **6**, 1201-1204.
47. T. Kim, E. J. Cho, Y. Chae, M. Kim, A. Oh, J. Jin, E. S. Lee, H. Baik, S. Haam, J. S. Suh, Y. M. Huh and K. Lee, *Angew Chem Int Edit*, 2011, **50**, 10589-10593.
48. S. H. Crayton and A. Tsourkas, *Acs Nano*, 2011, **5**, 9592-9601.
49. K. E. Lokling, S. L. Fossheim, J. Klaveness and R. Skurtveit, *J Control Release*, 2004, **98**, 87-95.
50. M. M. Ali, M. Woods, P. Caravan, A. C. L. Opina, M. Spiller, J. C. Fettinger and A. D. Sherry, *Chem-Eur J*, 2008, **14**, 7250-7258.
51. L. Barner, T. P. Davis, M. H. Stenzel and C. Barner-Kowollik, *Macromol Rapid Comm*, 2007, **28**, 539-559.
52. K. Wang, H. Peng, K. J. Thurecht, S. Puttick and A. K. Whittaker, *Polym Chem-Uk*, 2013, **4**, 4480.
53. G. Saito, J. A. Swanson and K. D. Lee, *Adv Drug Deliver Rev*, 2003, **55**, 199-215.
54. M. W. Jones, R. A. Strickland, F. F. Schumacher, S. Caddick, J. R. Baker, M. I. Gibson and D. M. Haddleton, *J Am Chem Soc*, 2012, **134**, 1847-1852.
55. A. W. Jackson and D. A. Fulton, *Macromolecules*, 2012, **45**, 2699-2708.
56. G. Moad, Y. K. Chong, A. Postma, E. Rizzardo and S. H. Thang, *Polymer*, 2005, **46**, 8458-8468.
57. Y. T. Li and S. P. Armes, *Macromolecules*, 2005, **38**, 8155-8162.
58. Q. Qiu, G. Y. Liu and Z. S. An, *Chem Commun*, 2011, **47**, 12685-12687.
59. X. F. Shi, W. Zhou, Q. Qiu and Z. S. An, *Chem Commun*, 2012, **48**, 7389-7391.
60. C. L. Zhang, M. Miao, X. T. Cao and Z. S. An, *Polym Chem-Uk*, 2012, **3**, 2656-2664.
61. X. F. Shi, M. Miao and Z. S. An, *Polym Chem-Uk*, 2013, **4**, 1950-1959.
62. J. Ferreira, J. Syrett, M. Whittaker, D. Haddleton, T. P. Davis and C. Boyer, *Polym Chem-Uk*, 2011, **2**, 1671-1677.
63. K. M. Yang, H. Liang and J. Lu, *J Mater Chem*, 2011, **21**, 10390-10398.
64. Z. M. Dong, X. H. Liu, H. W. Liu and Y. S. Li, *Macromolecules*, 2010, **43**, 7985-7992.
65. F. Cheng, E. M. Bonder, A. Doshi and F. Jakle, *Polym Chem-Uk*, 2012, **3**, 596-600.
66. A. Blencowe, J. F. Tan, T. K. Goh and G. G. Qiao, *Polymer*, 2009, **50**, 5-32.
67. F. H. Meng, W. E. Hennink and Z. Zhong, *Biomaterials*, 2009, **30**, 2180-2198.
68. A. H. Soeriyadi, G. Z. Li, S. Slavin, M. W. Jones, C. M. Amos, C. R. Becer, M. R. Whittaker, D. M. Haddleton, C. Boyer and T. P. Davis, *Polym Chem-Uk*, 2011, **2**, 815-822.
69. M. Li, P. De, H. M. Li and B. S. Sumerlin, *Polym Chem-Uk*, 2010, **1**, 854-859.
70. G. Y. Wu, Y. Z. Fang, S. Yang, J. R. Lupton and N. D. Turner, *J Nutr*, 2004, **134**, 489-492.
71. R. R. Perry, J. Mazetta, M. Levin and S. C. Barranco, *Cancer*, 1993, **72**, 783-787.
72. A. Russo, W. Degraff, N. Friedman and J. B. Mitchell, *Cancer Res*, 1986, **46**, 2845-2848.

This journal is © The Royal Society of Chemistry [year]